JOURNAL OF MATERIALS SCIENCE 24 (1989) 4275–4278

Pseudo-binary system Bi_2O_3–TeO_2 in air

TAKESHI KIKUCHI*, YOSHIZO KITAMI, MASATO YOKOYAMA
National Institute for Research in Inorganic Materials, Namiki 1-1, Tsukuba-shi, 305 Japan
HIROSHI SAKAI
Research Reactor Institute, Kyoto University, Kumatori-cho, Sennan-gun, Osaka, 590-04 Japan

The phase equilibria in the pseudo-binary system Bi_2O_3–TeO_2 at 600° ~ 950° C in air were examined by solid-state reaction techniques and X-ray powder diffraction method. Four pseudo-binary compounds appeared, i.e., δ-Bi_2O_3 type solid solution having a compositional range of $(1-x)Bi_2O_3 \cdot xTeO_2$ where $x = 0 \sim 0.4$ a new compound $Bi_6Te_2O_{15}$ which has an orthorhombic cell of $a = 2.27(4)$ nm, $b = 1.06(1)$ nm and $c = 0.539(8)$ nm, $2Bi_2O_3 \cdot 3TeO_2$, and an unidentified phase $Bi_2O_3 \cdot 2TeO_2$. The formation of the phase $Bi_6Te_2O_{15}$, in which all the Te ions are hexavalent, was confirmed by the thermogravimetry and by the Mössbauer spectra. The liquidus curves for whole system were determined by DTA method.

1. Introduction

High temperature modification of bismuth oxide (δ-Bi_2O_3) has an oxygen-deficient fluorite structure [1–4]. This phase exhibits an excellent oxygen ion conduction [5], though the phase is unquenchable and crystallizes above 730° C [3]. Addition of some other cations makes it possible to quench the phase [6–8]. Tellurium ion is known as one of those additives [9]. Phase diagram of the system Bi_2O_3–TeO_2 for Bi_2O_3 rich portion was studied by Levin and Roth [10]. The compounds in the whole system were reported by some investigators [9, 11, 12]. However there are some discrepancies among their data as shown in Table I. These might be caused by the difference of oxygen partial pressure (Po_2) equilibrated with sample at temperatures investigated. Frit *et al.* [9] used sealed gold tubes to prevent evaporation and oxidation of TeO_2 component. Even so, it seems to be inevitable that some Te^{+6} ions are introduced in the system.

In the present study, the samples were heated in air, where Po_2 was rather high and regarded as constant. As a result, our data differed from those of previous works.

2. Experimental procedure

Polycrystalline specimens of compositions in Bi_2O_3–TeO_2 were prepared by solid-state reactions. As starting materials, Bi_2O_3 and TeO_2, each 99.9% pure, were weighed in desired proportions and mixed in an agate mortar under ethanol. After drying, the mixtures were heated in a covered platinum crucible at 650°–850° C for 24 h in air and then cooled rapidly to room temperature. All the specimens were examined by X-ray powder diffraction (XRPD) using a conventional diffractometer with Ni-filtered Cu$K\alpha$ radiation. The results showed that reactions were completed at temperatures investigated. To determine liquidus curves in the phase diagram, differential thermal analyses (DTA) were made using a conventional DTA apparatus.

Electron diffraction patterns of an unknown phase were taken using a 500 kV electron microscope (H-500) equipped with a goniometer stage ($\pm 30°$ tilt). The polycrystalline samples were ground in acetone in an agate mortar. The powder obtained was mounted on a carbon mesh supporting film. The edge of a thin fragment of crystal, was projected over a hole, to tilt and rotate until it gave an expected diffraction pattern.

TABLE I Phases reported in the system Bi_2O_3–TeO_2

Demina and Dolgikh [12]			Frit *et al.* [9]		Crystal System [12]
Phase	Temp. (° C)	TeO_2 (mol %)	Temp. (° C)	TeO_2 (mol %)	
I	800	4–15	750	< 9.5	β-Bi_2O_3 type s.s.
II	800	16–34	750	12.3–33.3	δ-Bi_2O_3 type s.s.
III	650	28.5	not found		Orthorhombic
IV	650	40	750	38.46	Tetragonal
V	650	50–65	750	50–66.6	Orthorhombic
VI	650	66.6	not found		Tetragonal
VII	650	80	450	80	Monoclinic

Present address: Department of Geology and Mineralogy, Faculty of Science, Hokkaido University, Kitaku, Sapporo, 060 Japan.

0022–2461/89 $03.00 + .12

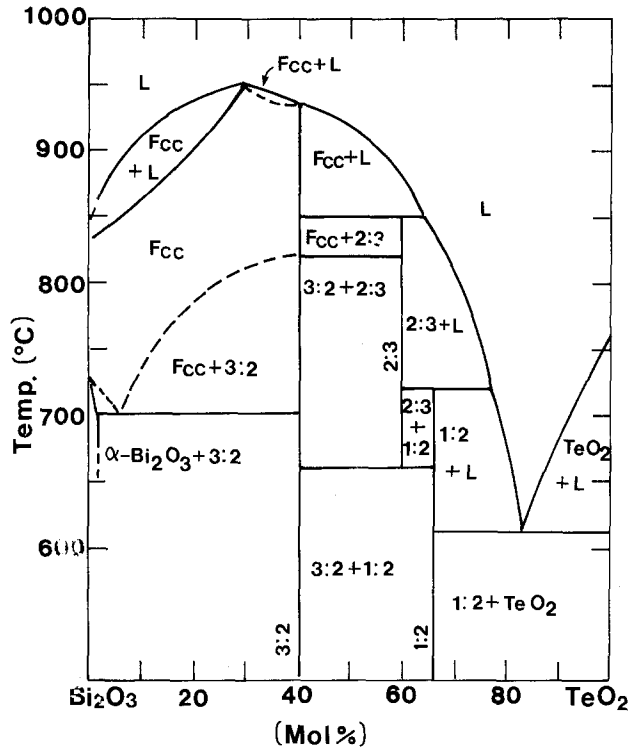

Figure 1 Phase diagram for the pseudo-binary system Bi_2O_3–TeO_2 in air. fcc, Face centered cubic phase; L, Liquid; Ratio m:n, $mBi_2O_3 \cdot nTeO_2$.

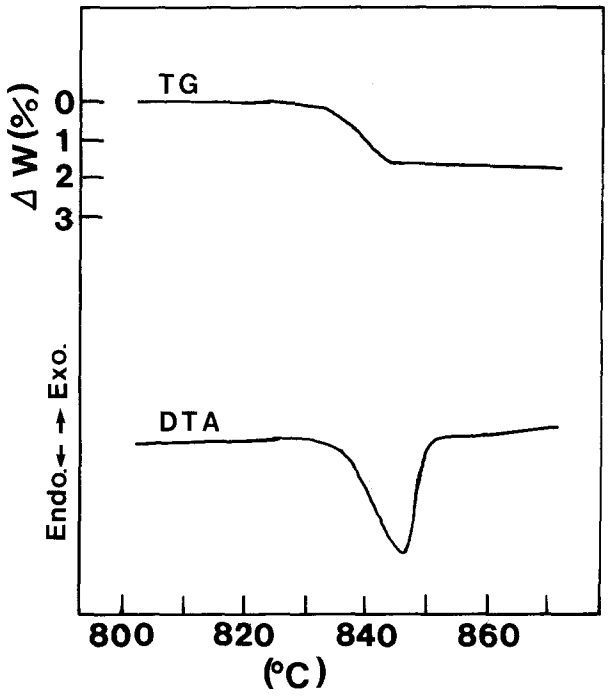

Figure 3 TG and DTA curves for $Bi_6Te_2O_{15}$ measured at a rate of 5° C min^{-1}.

The Mössbauer spectra of ^{125}Te in the phase "$3Bi_2O_3 \cdot 2TeO_2$" were measured in a transmission geometry by cooling a Mössbauer source and each absorber sample at 16 K with a closed-cycle helium refrigerator. $Cu^{125}I$ was used as the Mössbauer source of ^{125}Te. The isomer shift of the source has been determined to be -0.13 mm sec^{-1} relative to the ZnTe standard absorber [13]. The 35.5 keV Mössbauer γ-ray was detected indirectly by counting the 5.8 keV escaped peak in a Xe–CO_2 proportional counter.

3. Results and discussion

3.1. δ-Bi_2O_3 solid solution

Phase diagram of the pseudo-binary system Bi_2O_3–TeO_2 composed by the present data is given in (Fig. 1). β-Bi_2O_3 solid solution (phase I in Table I) obtained by heating the sample of 5 mol % TeO_2 at 750° C was neglected in the phase diagram since it was doubtful whether the phase obtained was equilibrated at the temperature investigated or the phase was brought by transformation of δ-Bi_2O_3 solid solution (fcc phase) within the time used for quenching.

fcc phase extends up to 40 mol % of TeO_2. The liquidus temperature increased with the increase of TeO_2 showing a maximum of 950° C at about 30 mol % of TeO_2. It was noticed that the quenched sample of the composition 80 mol % TeO_2 from its melt kept at 700° C was also fcc phase. The result implies that the liquid of this composition has a similar structure to fcc phase. The lattice parameters of fcc phase increased with the increase of TeO_2 (Fig. 2): it is indicated that the plots did not obey Vergards law. fcc phase of the limit composition (40 mol % TeO_2) were changed to the new phase $Bi_6Te_2O_{15}$ at temperatures lower than 830° C.

3.2. The phase $Bi_6Te_2O_{15}$

This phase was obtained at temperatures lower than

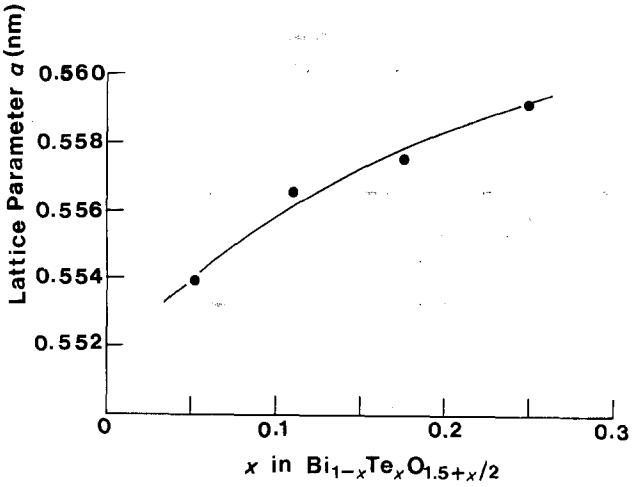

Figure 2 Variation of lattice parameter a of δ-Bi_2O_3 solid solution with x in $Bi_{1-x}Te_xO_{1.5+x/2}$.

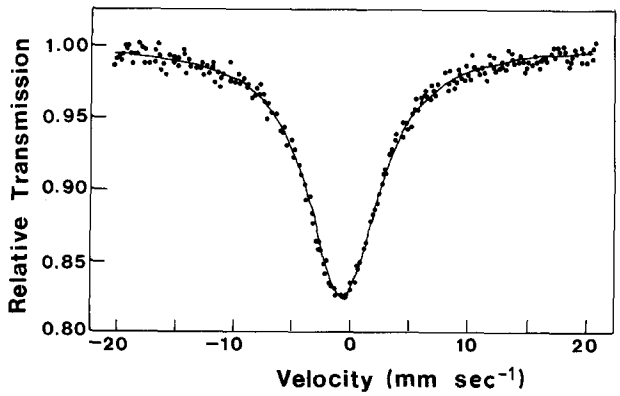

Figure 4 Mössbauer spectrum of polycrystalline $Bi_6Te_2O_{15}$ to the $Cu^{125}I$ source at 16 K.

830° C from the oxide mixture of $3Bi_2O_3 \cdot 2TeO_2$. The phase changed to fcc phase at about 830° C accompanying with a weight loss of 1.7 wt %. This value is comparable with the value (1.83 wt %) which is calculated on the assumption that all the tellurium atoms in the former phase are in the state of Te^{+6} and are reduced to Te^{4+} state accompanying deoxidation. The thermogravimetry (TG) and DTA data were shown in Fig. 3. The ^{125}Te Mössbauer spectra of the phase consist of a single peak with a small isomer shift ($-0.97\,mm\,sec^{-1}$) (Fig. 4). The result strongly suggests that the tellurium atoms in the phase exist exclusively as Te^{6+}, because the observed values of the isomer shift are close to those for β-TeO_3 ($-1.11\,mm\,sec^{-1}$) and Ca_3TeO_6 ($-1.06\,mm\,sec^{-1}$) [13–15]. From these data, it was concluded that the phase $3Bi_2O_3 \cdot 2TeO_2$ must be $Bi_6Te_2O_{15}$.

The X-ray diffraction data indicated a superstructure of fluorite, of which the unit cell is slightly distorted to orthorhombic symmetry. The electron diffraction patterns showed also strong spots derived from the fluorite subcell. A pattern which corresponds to the (0 0 1) reciprocal lattice section of fluorite subcell is shown in Fig. 5. It is shown that three weak spots are between the two strong spots along the [2 0 0] of fluorite subcell direction which is assumed to be horizontal to the paper and one weak spot is along the [0 2 0] of fluorite subcell. Taking XRPD data in consideration, an orthorhombic cell of $a \sim 4a_F$, $b \sim 2a_F$ and $c \sim a_F$, where a_F is the lattice parameter of the fluorite subcell, was most suitable to index the XRPD data. The precise lattice parameters of the orthorhombic cell for this phase were determined by the least-squares method using the foregoing preliminary lattice parameters, example being $a = 2.27(4)$ nm, $b = 1.060(9)$ nm and $c = 0.539(8)$ nm. Table II gives the observed d values, observed intensities, calculated

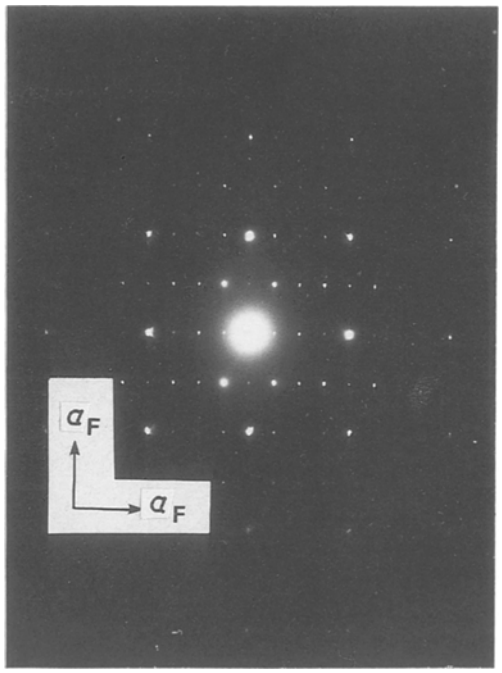

Figure 5 Electron diffraction pattern of $Bi_6Te_2O_{15}$. The electron beam is parallel to [001] of fluorite type subcell.

TABLE II XRPD data for $Bi_6Te_2O_{15}$ (Cu$K\alpha$)

d_{obs} (nm)	I/I_0	d_{calc} (nm)	hkl
0.567	2	0.5684	400
0.523	1	0.5252	101
0.515	2	0.5166	120
0.480	2	0.4807	220
0.433	5	0.4346	320
0.378	3	0.3789	600
0.367	5	0.3672	411
0.338	3	0.3385	321
0.314	100	0.3150	421
0.2909	3	0.2908	521
0.2841	60	0.2842	800
0.2783	5	0.2783	701
0.2699	30	0.2699	002
0.2653	25	0.2652	040
0.2633	2	0.2634	140
0.2626	2	0.2626	202
0.2614	3	0.2616	012
0.2438	1	0.2438	402
0.2404	1	0.2404	440
0.2391	2	0.2392	122
0.2367	1	0.2368	141
0.2293	3	0.2293	322
0.2281	1	0.2281	920
0.2146	3	0.2146	032
0.1956	30	0.1957	802
0.1939	30	0.1939	840
0.1926	6	0.1926	11, 2, 0
0.1921	6	0.1921	931
0.1892	25	0.1892	042
0.1694	40	0.1694	12, 2, 1
0.1642	2	0.1641	361
0.1632	30	0.1632	423
0.1612	25	0.1611	461
0.1574	23	0.1575	842

TABLE III XRPD data for "$Bi_2O_3 \cdot 2TeO_2$" (Cu$K\alpha$)

d (nm)	I/I_0	d (nm)	I/I_0
0.819	3	0.2103	6
0.579	2	0.2090	4
0.477	4	0.2058	2
0.471	6	0.2006	20
0.465	4	0.1937	10
0.411	7	0.1914	5
0.337	8	0.1907	8
0.326	3	0.1886	15
0.321	7	0.1855	4
0.316	95	0.1797	1
0.314	100	0.1787	1
0.310	11	0.1774	3
0.2894	50	0.1728	10
0.2831	1	0.1713	8
0.2772	30	0.1698	6
0.2730	2	0.1670	8
0.2653	8	0.1667	12
0.2560	20	0.1656	1
0.2488	1	0.1647	1
0.2455	2	0.1596	2
0.2392	3	0.1589	8
0.2285	3	0.1579	6
0.2201	< 1	0.1573	6
0.2146	4	0.1555	< 1
0.2127	4		

d values and Miller indices of XRPD lines for $Bi_6Te_2O_{15}$.

3.3. Conclusion

The XRPD data of the orthorhombic phase $2Bi_2O_3 \cdot 3TeO_2$ were almost the same as the phase V shown in Table I but its solid solution was not observed. This phase was stable in the temperature range of 850° to 670° C and decomposed to the assemblage of phases $Bi_6Te_2O_{15}$ and "$Bi_2O_3 \cdot 2TeO_2$" at temperatures lower than 670° C.

The phase "$Bi_2O_3 \cdot 2TeO_2$" was detected below 720° C. Though the composition of the phase was the same as the phase VII in Table I, its XRPD data given in Table III were different from previously reported [9, 12]. The phase might include Te^{6+} ions like the case of $Bi_6Te_2O_{15}$. To clarify the phase equilibrium relations in the complete Bi_2O_3–TeO_2–TeO_3 system, further experiments under precise control of Po_2 will be needed.

References

1. L. G. SILLEN, *Ark. Kemi. Mineral. Geol.* **12A** (1937) 1.
2. G. GATTOW and H. SCHROEDER, *Z. Anorg. Allg. Chem.* **318** (1962) 176.
3. J. W. MEDERNACH and R. L. SNYDER, *J. Amer. Ceram. Soc.* **61** (1978) 494.
4. H. A. HARWIG, *Z. Anorg. Allg. Chem.* **444** (1978) 151.
5. C. N. R. RAO, G. V. SUBBA RAO and S. RAMDAS, *J. Phys. Chem.* **75** (1969) 672.
6. T. TAKAHASHI, H. IWAHARA and T. ARAO, *J. Appl. Electrochem.* **5** (1975) 187.
7. T. TAKAHASHI, T. ESAKA and H. IWAHARA, *J. Appl. Electrochem.* **5** (1977) 197; **7** (1977) 299; **7** (1977) 303.
8. M. J. VERKERK, G. M. H. VAN DE VELDE and A. J. BUGGRAAF, *J. Phys. Chem. Solids* **43** (1982) 1129.
9. B. FRIT, M. JAYMES, G. PEREZ, and P. HAGENMULLER, *Rev. Chim. miner.* **8** (1971) 453.
10. E. M. LEVIN and S. ROTH, *J. Res. Natl. Bur. Stand.* **68A** (1964) 201.
11. B. FRIT, and M. JAYMES, *Rev. Chim. miner.* **9** (1972) 837.
12. L. A. DEMINA and V. A. KOLGIKH, *Rus. J. Inorg. Chem.* **29** (1984) 547.
13. H. SAKAI and Y. MAEDA, *Bull. Chem. Soc. Japan* **62** (1989) 33.
14. M. TAKEDA and N. N. GREENWOOD, *J. Chem. Soc. Dalton Trans.* (1975) 2207.
15. P. DOBUD and C. H. W. JONES, *J. Solid State Chem.* **16** (1976) 201.

Received 29 July 1988
and accepted 15 January 1989